Monitoring Picoliter Sessile Microdroplet Dynamics Shows That Size Does Not Matter

I. Rodriguez-Ruiz, Z. Hammadi, R. Grossier, J. Gomez-Morales, S. Veesler

Monitoring picoliter sessile microdroplet dynamics shows that size doesn't matter

Isaac Rodríguez-Ruiz[a], Zoubida Hammadi[b], Romain Grossier[b], Jaime Gómez-Morales[a,] and Stéphane Veesler[b,]*

[a]*Laboratorio de Estudios Cristalográficos, IACT (CSIC-UGR). Avda. de las Palmeras, 4. 18100 Armilla, Granada, Spain.*

[b] *CINaM-CNRS, Aix-Marseille Université, Campus de Luminy F-13288 Marseille, France*

Phone : 336 6292 2866, Fax : 334 9141 8916, veesler@cinam.univ-mrs.fr

ABSTRACT: We monitor the dissolution of arrayed picoliter-size sessile microdroplets of aqueous phase in oil, generated using a recently developed fluidic device. Initial pinning of the microdroplet perimeter leads to a nearly constant contact diameter; thus contraction proceeds via microdroplet (micrometer diameter) height and contact angle reductions. This confirms that picoliter microdroplets contraction or dissolution due to selective diffusion of water in oil has comparable dynamics with microliter droplets evaporation in air. We observe a constant microdroplet dissolution rate in different aqueous solutions. The application of this simple model to solvent-diffusion-driven crystallization experiments in confined volumes, for instance, would allow us to precisely determine the concentration in the microdroplet during an experiment and particularly at nucleation.

INTRODUCTION

Numerous applications involve reducing droplet volume with time : drying of colloidal suspension[1], drying of human blood drops for diagnostic purposes[2], coffee ring deposition on solid surfaces[3], efficacy and efficiency of pesticide application[4], meteorology and air-conditioning [5], nanoscale pipetting for confined

chemistry[6], detection of molecules and biomarkers below picomolar concentration[7], deterioration of building materials[8-9] (due to salt crystallization in the pores), ink-jet-based direct writing technology[10], crystallization of protein [11], and crystallization in confined environments[12-13]. Understanding how droplet volume can be reduced means looking at the dynamics of droplet evaporation, drying, dissolution or contraction for geometries ranging from aerosol to sessile and sizes ranging from millimeter to micrometer. Sessile droplet evolution can be characterized by monitoring over time the contact angle of the droplet with the substrate, the droplet height and the contact diameter. Thus, evaporation of a sessile droplet in the microliter range is known to proceed through different modes: constant contact angle, constant contact area and mixed mode, depending on surface roughness and chemical nature, atmospheric conditions and droplet size[14-17] It is although of interest to consider picoliter droplets (micrometer diameter), to check model validity at this scale, there is little references to this in the literature[18-21]. Most experiments are performed with microliter droplets (millimeter diameter), mainly due to the rapid evaporation of such small microdroplets, rendering quantitative measurements difficult. In this context, it has proved challenging to perform quantitative monitoring of droplet dynamics in the micrometer range: the smaller the droplet, the faster the dynamics. While fast imaging may have potential, there are still limitations regarding accuracy of measurement of the first instants of these droplet dynamical. In this letter we use the term "microdroplets" for droplets in the micrometer range and "droplets" for droplets in the millimeter range.

Recently, we presented a simply-constructed and easy-to-use fluidic device that generates arrayed aqueous phase microdroplets under oil (sessile geometry), with volumes ranging from nanoliter to femtoliter, without surfactant[22]. In subnanoliter experiments performed with this fluidic device, we observed contraction of NaCl microdroplets[23] due to selective diffusion of water into oil[24], which acts as a buffer to slow down the diffusion rate. This process generates an increment of solute concentration and thus, supersaturation, ensuring crystallization. This application illustrates the potential of this technology in the field of particle generation, where small volume systems offer promising properties[12-13]. Microdroplets were observed under an inverted optical microscope and the solute concentration was qualitatively monitored through the evolution of the optical contrast between the droplet and the continuous phase. For a more precise and quantitative determination of the solute concentration during the diffusion process, it should be possible to

monitor the droplet volume. This was performed, for instance, by image analysis of dispersed aqueous salt solutions in silicone oil[24-25], but not for sessile microdroplets.

Here, in order to measure solute concentration, we perform experiments in which the contraction of sessile microdroplets of aqueous phase into oil is observed using an optical microscope. Contact angle of the microdroplet with the substrate, microdroplet height and contact diameter are monitored during diffusion of water into oil and, using simple trigonometry presented in the APPENDIX, microdroplet volumes are computed. We observe a constant microdroplet dissolution rate whatever the microdroplet composition. In this letter, we show that this microdroplet contraction or dissolution due to selective diffusion of water in oil is equivalent to the evaporation of a droplet in air in a stationary diffusion-controlled evaporation with local equilibrium at the drop interface[16].

EXPERIMENTAL

Microdroplets are generated[22] under an optical microscope (Zeiss Axio Observer D1) by a microinjector (Femtojet, Eppendorf) on a plastic coverslip (22x22mm SPI) covered with approximately 100µL of paraffin oil (HR3-421) and inserted in a home-made plastic cell with vertical walls for side observation using an optical microscope. The cell is, then, transferred and observed under a side-view microscope (Olympus BXFM focusing module equipped with a home-made holder) (figure 1). Here the solution is a 2.71M NaCl aqueous solution, half the solubility of NaCl in water at 20°C[26], see Supplementary File for solution preparation.

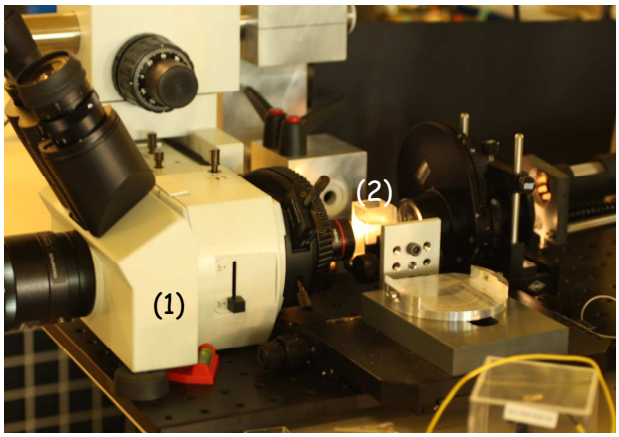

Figure.1. Image of the experimental setup for side observation**,** (1) microscope and (2) plastic cell.

Figure 2 presents top and side views of a part of an array of 2.71M NaCl microdroplets in oil. In a previous paper, we showed the monodispersity of the droplet size at the pixel resolution[22]. For instance, the volume of the 4 microdroplets in figure 2b is 151±7pL (details of the calculation are given in APPENDIX).

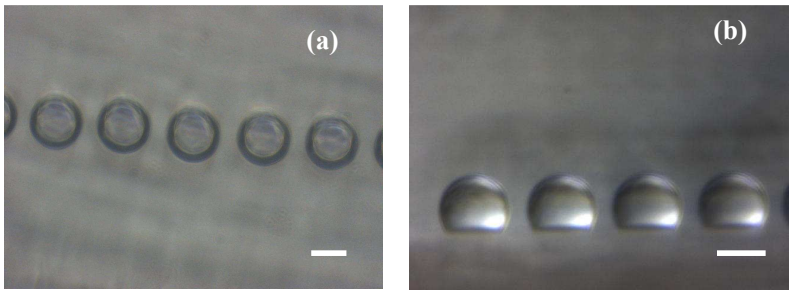

Figure 2. (a) Top view and (b) side view of 2.71M NaCl microdroplets (151pL) in oil. The scale bar represents 50µm.

RESULTS AND DISCUSSIONS

The sequence in figure 3 presents the 2.71M NaCl microdroplet contraction by diffusion of water into oil. During contraction, the solution becomes increasingly concentrated. At the end of the process, when the concentration reached instability, the microdroplets collapse due to the nucleation and growth of one single crystal per microdroplet in accordance with our theoretical prediction[27]. One example of an application this phenomenon is its use to deposit a solute in a confined region [7].

In practice, because of the microdroplet size, we can assume there is no shape distortion due to gravity; this is confirmed by the value of the Bond number of $3.7\ 10^{-6}$ for a microdroplet of 100µm diameter[28]. Thus microdroplet profiles can be fitted to a segment of a circle[14, 18]. Thus contact angle of the microdroplet with the substrate, microdroplet height and contact diameter can be easily extracted from this experiment (fig. 4 and in supplementary file at URL).

Contact angle (fig.4a): Evaporation of a sessile droplet is known to proceed through different modes as mentioned above. Figure 4a shows a continuous decrease of the contact angle, θ. The initial contact angle can be identified as an advancing angle (θ_A), which decreases until it reaches the receding angle (θ_R), thus :

$$\theta_A > \theta > \theta_R \quad (1)$$

This decrease is the "stage II" described by Bourgès-Monnier and Shanahan[15], where height and contact angle decrease, while contact diameter remains constant (also known in the literature as the constant contact diameter mode or CCD mode). At the end of the stage II, the contact angle is θ_R and should remain constant, although this is not observed here because nucleation has already occurred (fig.3f-i).

s

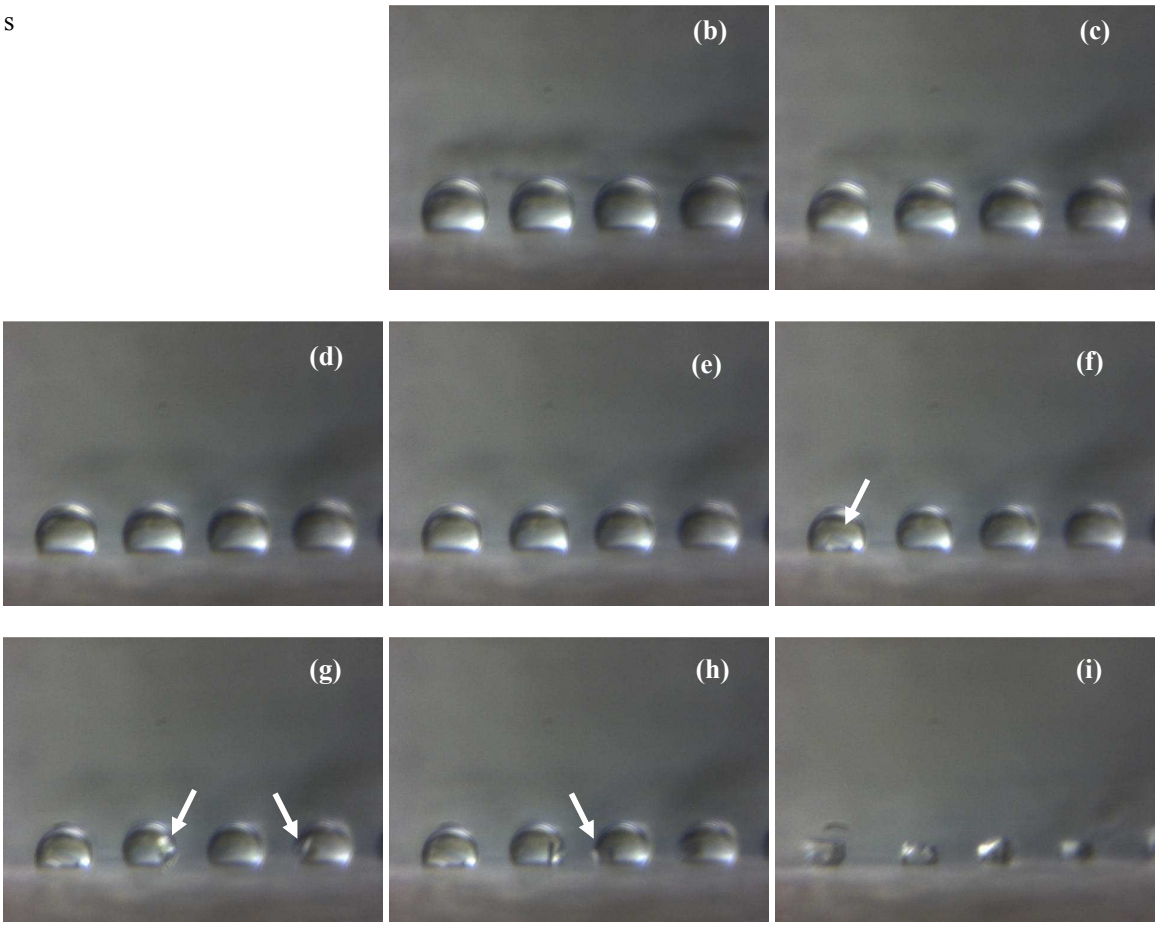

Figure.3. Time sequence showing the side view of 2.71M NaCl microdroplets (151pL) contraction in oil, (a) t=0min, (b) t=60.05min, (c) t=130.12min, (d) t=190.18min, (e) t=260.25min, (f) t=330.32min (g) t=360.32min, (h) t=380.32min and (i) t=740.31min. Arrows in (f), (g) and (h) show crystals. See Supplementary material for a movie of this process.

Height and contact diameter (fig.4b): The evolution of these parameters confirms that the process is in stage II. An initial pinning of the perimeter leads to a nearly constant contact diameter (respectively area), thus contraction proceeds via microdroplet height and contact angle reductions[18]. These results confirm that evaporation of picoliter microdroplets is comparable to that of microliter droplets. Moreover, the rapid

decrease in θ in the first stage due to rapid evaporation in air observed by Taylor et al.[18] is not observed, because the oil acts as a buffer. As stated by Duncan and Needham[29], compared to pure gas-liquid systems (air-water), pure liquid-liquid (oil-water) systems have higher densities (~1000X), lower diffusion constants (~10X), lower solubility-limit concentrations (~100X); therefore dissolution lifetime can vary from seconds to hours. For instance, in previous experiments presented by Furuta[19], evaporation of a 800pL droplet in air takes about 8s, whereas here, evaporation takes several hours.

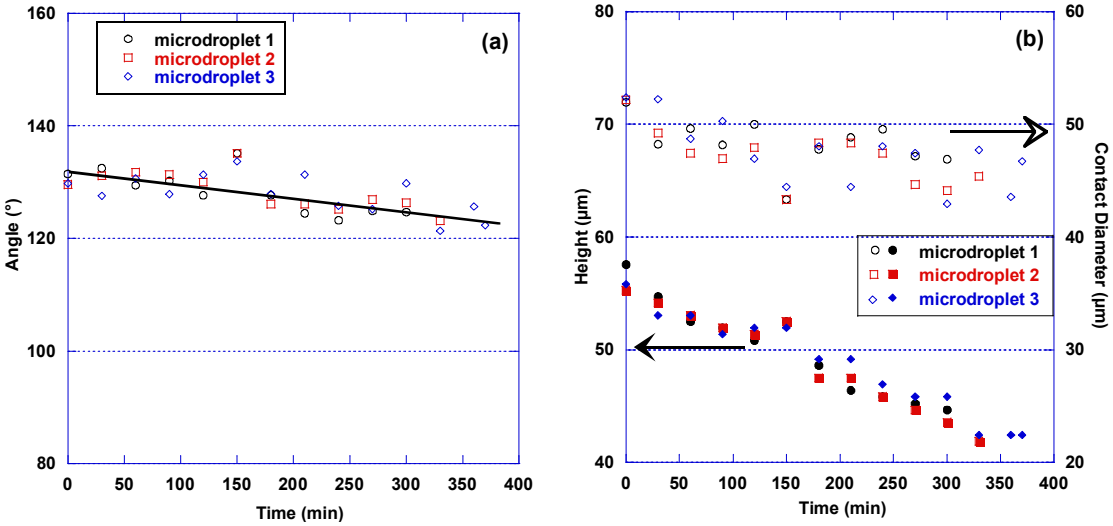

Figure 4: (a) Contact angle of the microdroplets with the substrate and (b) microdroplet height and contact diameter. The line is a guide to the eyes and microdroplet are from figure 3.

Volume contraction (fig.5): Figure 5 presents the evolution of NaCl-, water-, Na_2CO_3- and $CaCl_2$-microdroplet volumes with time; lines are linear fits of the data corresponding to a constant microdroplet dissolution rate (equation (2)).

$$\frac{V}{V_0} = (1 - \alpha \times t) \qquad (2)$$

with V_0 and V the initial and time t microdroplet volumes respectively and α the normalized dissolution rate; α is a linear function of the saturation fraction of water in oil[29]. A semi-log plot is used in figure 5b and d to

illustrate the apparent final acceleration in the evaporation, which is not due to an increase in the evaporation rate but to the fact that there is less matter to evaporate.

The dissolution rate of a water microdroplet into an infinite medium is known to be constant. In our experiments, water microdroplets of 64.6pL (±1.2) are formed in an immiscible medium having a volume of ~100 µL (6 orders of magnitude larger than the microdroplets), which means that the water droplet is in an effectively infinite dilution regime, as confirmed by the constant value of α obtained in our experiments in pure water (fig.5a). Moreover, when a salt is added to water the rate of solvent dissolution will be constant for a dilute solution if the activity of water is not greatly affected by the presence of salt. In their paper, Talreja et al.[30] assumed a constant evaporation rate for protein and salt solutions until $\frac{V}{V_0} = 0.15$. In our experiments with 2.71M NaCl solutions (fig.5a and b) the dissolution rate is constant until nucleation occurs for $\frac{V}{V_0} > 0.4$, in agreement with Talreja et al. Moreover, the dissolution rate is also constant for Na_2CO_3- and $CaCl_2$-microdroplets dissolution.

It is well-known that a constant total evaporation rate and a volume decreasing linearly with time at constant contact diameter is observed for the evaporation of a sessile droplet in quiescent open air in partial wetting, if the contact line is pinned[3, 14, 16, 31]. This is the case in our experiments. Therefore, the overall behavior of microdroplet dissolution is identical to that of a stationary diffusion-controlled evaporation with local equilibrium at the drop interface[16]. Note that at the very end of the process, for V/V0<0.1 in the case of water microdroplets (fig.5a and b and fig. S2 in supplementary file at URL), this simple model no longer works.

Lastly, we tested the modified model of Picknett and Bexon[14] by McHale et al.[32] for CCD mode with diffusion-controlled evaporation (equation 20 in reference[32] and supplementary file at URL). This model, valid only for θ≥90° as in our experiments, gives the diffusion constant –concentration difference product estimation in agreement with the literature (supplementary file at URL).

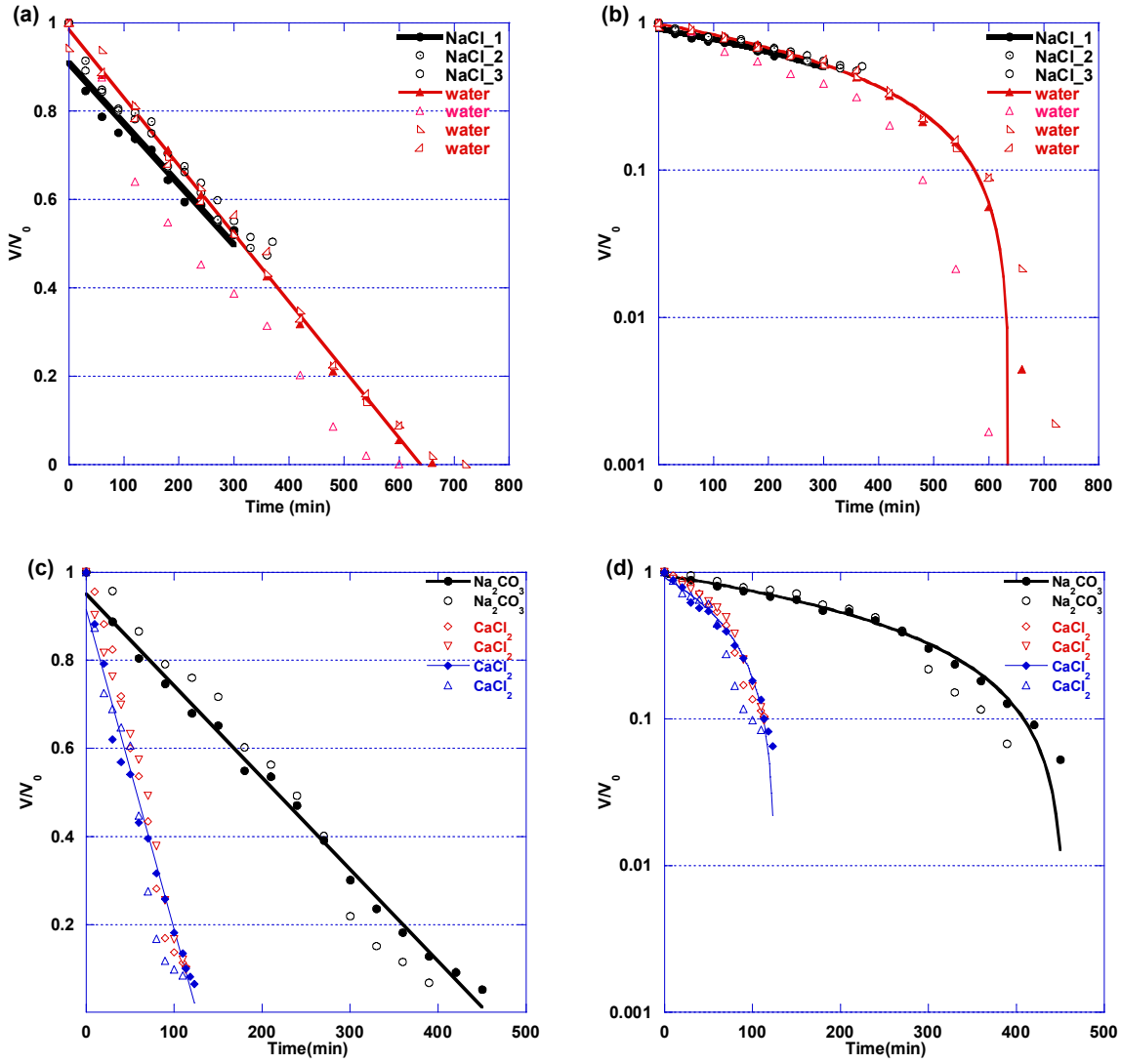

Figure 5: Volume contraction in linear and semi-log plots (a) and (b) for the 2.71M NaCl and water microdroplets of initial volume of 151pL (±7) and 64.6pL (±1.2) respectively and (c) and (d) for 60mM Na_2CO_3 and $CaCl_2$ microdroplets of initial volume of 655pL (±24) and 42.2pL (±5.5) respectively. NaCl microdroplets are from figure 3; lines are linear fits of the data.

In conclusion, we present experiments in which the contraction of sessile microdroplets of aqueous phase in oil is monitored using a recently developed[22] fluidic device that generates arrayed aqueous phase microdroplets in oil. An initial pinning of the microdroplet perimeter leads to a nearly constant contact diameter; thus contraction proceeds via microdroplet height and contact angle reductions. This confirms the process to be the stage II described by Bourgès-Monnier and Shanahan[15] for evaporation of a sessile droplet

corresponding to a stationary diffusion-controlled evaporation with local equilibrium at the drop interface[16]. Thus, microdroplets (micrometer diameter) behave like droplets. We observed a constant dissolution rate of the microdroplet for pure water and in different salts. The application of this simple model to solvent-diffusion-driven crystallization experiments in confined volumes, for instance, would allow us to precisely determine the concentration in the microdroplet during an experiment and particularly at nucleation.

ACKNOWLEDGEMENTS

This work was carried out within the framework of the project MAT2011-28543 (Spanish MINECO). J.G.M. and I.R.R. belong to the research team "Factoría de Cristalización" (Consolider Ingenio 2010) of the Spanish Ministerio de Ciencia e Innovación. IRR also acknowledges CSIC for his contrat JAE-Pre cofunded by the European Social Fund. The authors thank Professor Juan Manuel García-Ruiz for supporting I.R.R. and encouraging him to perform this research. We thank M. Sweetko for English revision.

SUPPORTING INFORMATION

Reagents and solutions, graph of contact angle, height and contact diameter for water microdroplets, time sequence of volume contraction for water microdroplets, test of constant contact radius mode with diffusion-controlled evaporation and computing contact angle of the microdroplet with the substrate, microdroplet height, contact diameter and microdroplet volumes.

Video showing the side view of 2.71M NaCl microdroplets contraction in oil.

This information is available free of charge via the Internet at http://pubs.acs.org/

REFERENCES

(1) Parisse, F.; Allain, C., Drying of Colloidal Suspension Droplets: Experimental Study and Profile Renormalization. *Langmuir* **1997,** *13* (14), 3598-3602.
(2) Brutin, D.; Sobac, B.; Loquet, B.; Sampol, J., Pattern formation in drying drops of blood. *Journal of Fluid Mechanics* **2011,** *667*, 85-95.
(3) Deegan, R., D.; Bakajin, O.; Dupont, T., F.; Huber, G.; Nagel, S. R.; Witten, T., A., Capillary flow as the cause of ring stains from dried liquid drops. *Nature* **1997,** *389*, 827-829.
(4) Yu, Y.; Zhu, H.; Frantz, J. M.; Reding, M. E.; Chan, K. C.; Ozkan, H. E., Evaporation and coverage area of pesticide droplets on hairy and waxy leaves. *Biosystems Engineering* **2009,** *104* (3), 324-334.
(5) Houghton, H. G., A Study of the Evaporation of Small Water Drops. *Physics* **1933,** *4* (12), 419-424.
(6) Rodolfa, K. T.; Bruckbauer, A.; Zhou, D.; Schevchuk, A. I.; Korchev, Y. E.; Klenerman, D., Nanoscale Pipetting for Controlled Chemistry in Small Arrayed Water Droplets Using a Double-Barrel Pipet. *Nano Letters* **2006,** *6* (2), 252-257.
(7) De Angelis, F.; Gentilef; Mecarinif; Dasg; Morettim; Candelorop; Coluccio, M. L.; Cojocg; Accardoa; Liberalec; Zaccaria, R. P.; Perozziellog; Tirinatol; Tomaa; Cudag; Cingolanir; Di Fabrizio, E., Breaking the diffusion limit with super-hydrophobic delivery of molecules to plasmonic nanofocusing SERS structures. *Nat Photon* **2011,** *5* (11), 682-687.
(8) Winkler, E. M.; Singer, P. C., Crystallization Pressure of Salts in Stone and Concrete. *Geological Society of America Bulletin* **1972,** *83* (11), 3509-3514.
(9) Shahidzadeh-Bonn, N.; Desarnaud, J.; Bertrand, F.; Chateau, X.; Bonn, D., Damage in porous media due to salt crystallization. *Physical Review E* **2010,** *81* (6), 066110.
(10) Hon, K. K. B.; Li, L.; Hutchings, I. M., Direct writing technology--Advances and developments. *CIRP Annals - Manufacturing Technology* **2008,** *57* (2), 601-620.
(11) Ducruix, A.; R. Giégé, *Crystallization of Nucleic Acids and Proteins*

A Practical Approach second ed.; Oxford University Press: Oxford, 1999; p 460.
(12) Lee, A. Y.; Lee, I. S.; Dette, S. S.; Boerner, J.; Myerson, A. S., Crystallization on Confined Engineered Surfaces: A Method to Control Crystal Size and Generate Different Polymorphs. *J. Am. Chem. Soc.* **2005,** *127* (43), 14982-14983.
(13) Grossier, R.; Hammadi, Z.; Morin, R.; Veesler, S., Predictive Nucleation of Crystals in Small Volumes and Its Consequences. *Physical Review Letters* **2011,** *107* (2), 025504.
(14) Picknett, R. G.; Bexon, R., The evaporation of sessile or pendant drops in still air. *Journal of Colloid and Interface Science* **1977,** *61* (2), 336-350.
(15) Bourges-Monnier, C.; Shanahan, M. E. R., Influence of Evaporation on Contact Angle. *Langmuir* **1995,** *11* (7), 2820-2829.
(16) Cazabat, A.-M.; Guena, G., Evaporation of macroscopic sessile droplets. *Soft Matter* **2010,** *6* (12), 2591-2612.
(17) Hu, H.; Larson, R. G., Analysis of the Microfluid Flow in an Evaporating Sessile Droplet. *Langmuir* **2005,** *21* (9), 3963-3971.
(18) Taylor, M.; Urquhart, A. J.; Zelzer, M.; Davies, M. C.; Alexander, M. R., Picoliter Water Contact Angle Measurement on Polymers. *Langmuir* **2007,** *23* (13), 6875-6878.
(19) Furuta, T.; Sakai, M.; Isobe, T.; Nakajima, A., Evaporation Behavior of Microliter- and Sub-nanoliter-Scale Water Droplets on Two Different Fluoroalkylsilane Coatings. *Langmuir* **2009,** *25* (20), 11998-12001.
(20) Arcamone, J.; Dujardin, E.; Rius, G.; Pérez-Murano, F.; Ondarçuhu, T., Evaporation of Femtoliter Sessile Droplets Monitored with Nanomechanical Mass Sensors. *The Journal of Physical Chemistry B* **2007,** *111* (45), 13020-13027.
(21) Talbot, E. L.; Berson, A.; Brown, P. S.; Bain, C. D., Evaporation of picoliter droplets on surfaces with a range of wettabilities and thermal conductivities. *Physical Review E* **2012,** *85* (6), 061604.
(22) Grossier R.; Hammadi Z.; Morin R.; Magnaldo A.; Veesler S, Generating nanoliter to femtoliter microdroplets with ease. *Applied Physics Letters* **2011,** *98* (9), 091916-3.
(23) Grossier R.; Magnaldo A.; Veesler S, Ultra-fast crystallization due to Confinement. *J. Crystal Growth* **2010,** *312*, 487-489.

(24) Velazquez J. A.; Hileman Jr O.E., Studies on nucleation from solution of some soluble inorganic salts. *Can. J. Chem.* **1970,** *48*, 2896-2899.
(25) Bempah O. A.; Hileman Jr. O. E., Mean Lifetime of an Embryo in the Homogeneous Nucleation from Solution of the Tetracyanoplatinates(II) of Barium, Calcium, and Magnesium. *Can. J. Chem.* **1973,** *51* (20), 3435-3442.
(26) Langer, H.; Offermann, H., On the solubility of sodium chloride in water. *Journal of Crystal Growth* **1982,** *60* (2), 389-392.
(27) Grossier R.; Veesler S., Reaching one single and stable critical cluster through finite sized systems. *Cryst. Growth Des.* **2009,** *9* (4), 1917-1922.
(28) Gaitzsch, F.; Gäbler, A.; Kraume, M., Analysis of droplet expulsion in stagnant single water-in-oil-in-water double emulsion globules. *Chemical Engineering Science* **2011,** *66* (20), 4663-4669.
(29) Duncan, P. B.; Needham, D., Microdroplet Dissolution into a Second-Phase Solvent Using a Micropipet Technique: Test of the Epstein−Plesset Model for an Aniline−Water System. *Langmuir* **2006,** *22* (9), 4190-4197.
(30) Talreja, S.; Kenis, P. J. A.; Zukoski, C. F., A Kinetic Model To Simulate Protein Crystal Growth in an Evaporation-Based Crystallization Platform. *Langmuir* **2007,** *23* (8), 4516-4522.
(31) Deegan, R. D., Pattern formation in drying drops. *Physical Review E* **2000,** *61* (1), 475 -485.
(32) Mchale, G.; Aqil, S.; Shirtcliffe, N. J.; Newton, M. I.; Erbil, H. Y., Analysis of Droplet Evaporation on a Superhydrophobic Surface. *Langmuir* **2005,** *21* (24), 11053-11060.

Supporting Information for: ***Monitoring picoliter sessile microdroplet dynamics shows that size doesn't matter***

Isaac Rodríguez-Ruiz, Zoubida Hammadi, Romain Grossier, Jaime Gómez-Morales and Stéphane Veesler*

Reagents and solutions

Sodium chloride (NaCl, ACS reagent, ≥ 99,0 % purity), calcium chloride dihydrate ($CaCl_2 \cdot 2H_2O$, Bioxtra, ≥ 99,0 % purity) and sodium carbonate monohydrate ($Na_2CO_3 \cdot H_2O$, ACS reagent, 99.5% purity) were supplied by Sigma-Aldrich.Sodium. Paraffin oil was supplied by Hampton Research. Density of 2.64M NaCl and of Paraffin oil are 1100.9kg/m^3 and 860 kg/m^3 respectively at 20°C.

Ultrapure water (0.18 µS, 25 °C, MilliQ©, Millipore) was used to prepare all the solutions. Solutions were filtered by using 0.22 µm Millipore filters.

Contact angle, height and contact diameter for water microdroplets of initial volume of 64.6pL (±1.2)

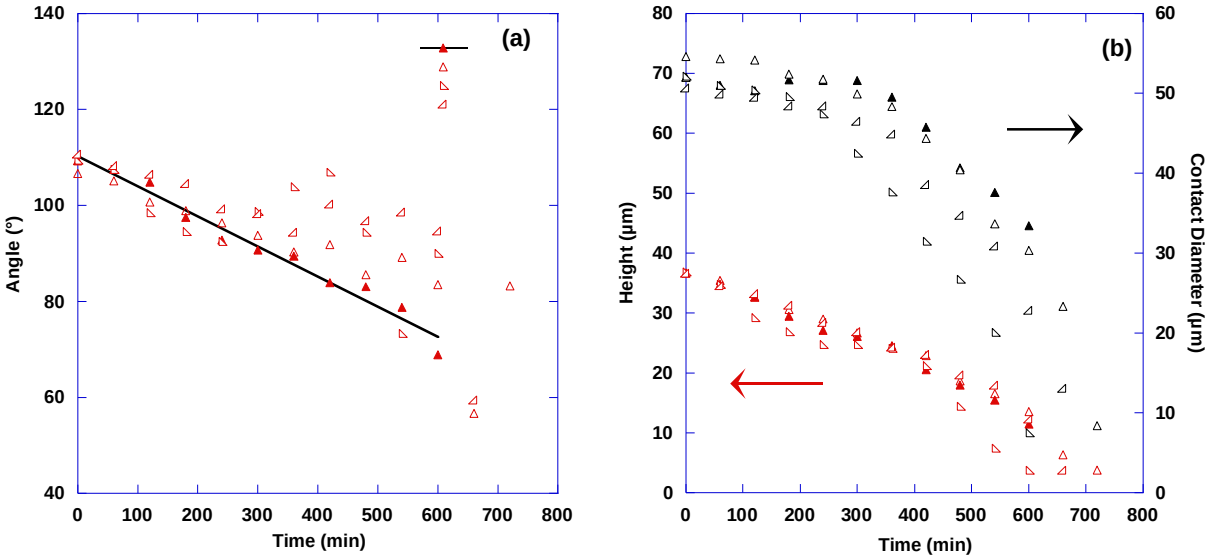

Figure S1: Time evolution of water microdroplets of initial volume of 64.6pL (±1.2) respectively (a) Contact angle of the microdroplets with the substrate and (b) microdroplet height and contact diameter. The line is a guide to the eyes.

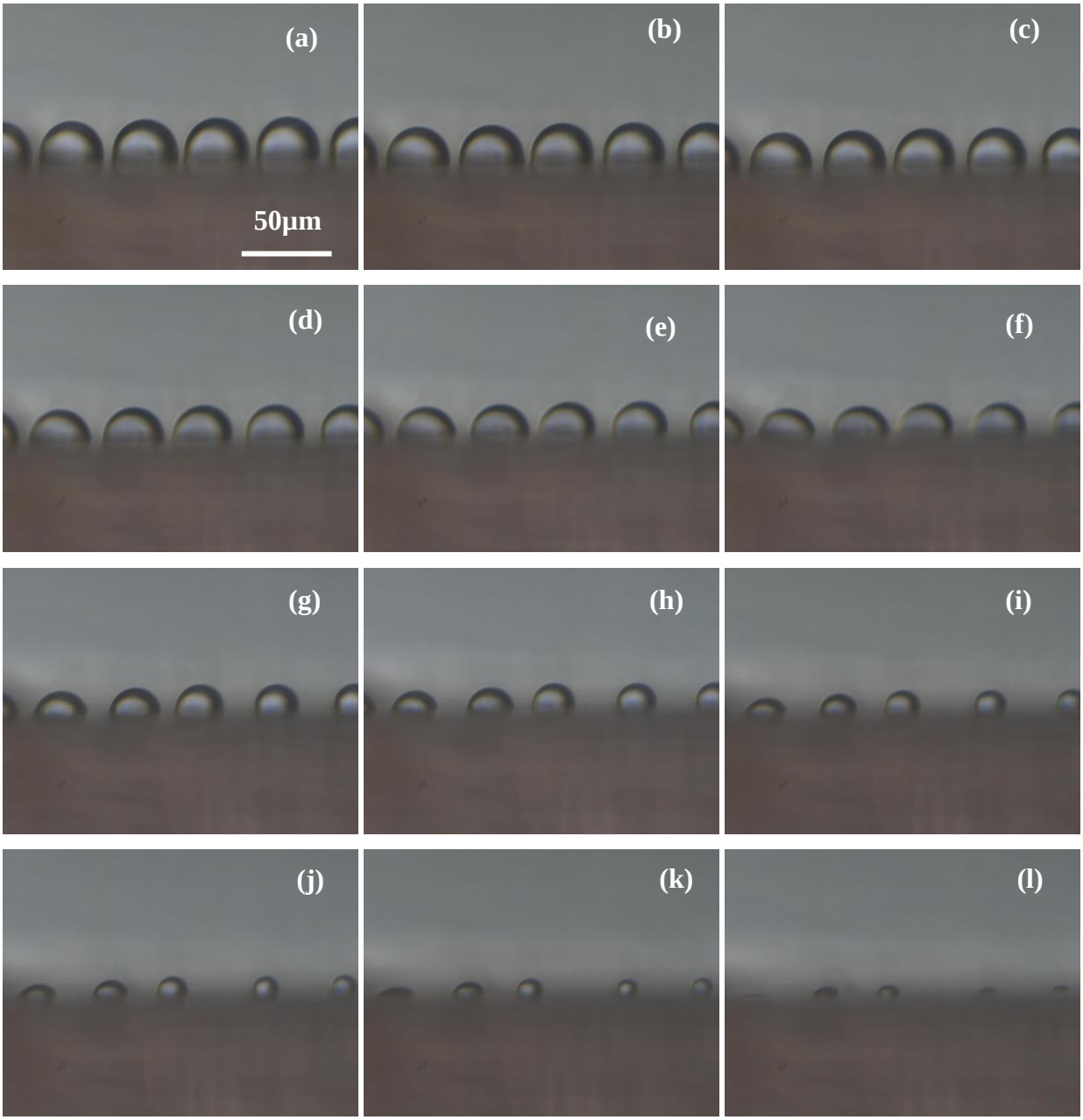

Figure S2. Time sequence showing the side view of water microdroplets (64.6pL) contraction in oil, (a) t=0min, (b) t=70min, (c) t=140min, (d) t=210 min, (e) t=280min, (f) t=350min (g) t=420min, (h) t=490min, (i) t=560min, (j) t=600min, (k) t=630min and (l) t=660min.

Test of constant contact radius mode with diffusion-controlled evaporation

Picknett and Bexon[1] gave an exact equation for the rate of mass loss of a sessile droplet of radius R and volume V:

$$\rho_L \times \frac{dV}{dt} = -4 \times \pi \times R \times D_{wo} \times \Delta c \times f(\theta) \qquad \text{(S1)}$$

with ρ_L the liquid density, D_{wo} the diffusion coefficient of water in oil, Δc $(=c_s - c_\infty)$ the difference between the concentration at the interface (assumed to be equal to the saturation concentration, c_s) and the ambient value far removed from the surface (c_∞), and $f(\theta)$ is a function of the contact angle taking in consideration the presence of the substrate which reduces the diffusion rate. McHale et al.[2] proposed an analytical form that is linear with time in the case of constant contact radius mode (with diffusion-controlled evaporation) :

$$\frac{\rho_L \times D^2 \times H_{PB}(\theta)}{8} = -D_{wo} \times \Delta c \times t + Cte \qquad \text{(S2)}$$

with D the contact diameter and $H_{PB}(\theta)$ the analytical function (see reference[2]) resulting of the integration of $f(\theta)$. Figure S3 shows the left hand term of (S2) in function of the time (t). From the slope we obtain $D_{wo}\Delta c = 1.3549\ 10^{-11}$ kg.m^{-1}.s^{-1}

Unfortunately, there is no data in the literature concerning the solubility and diffusivity of water in paraffin oil (paraffin oil supplied by Hampton Research is a mixture of different paraffin with carbon number, n, between 16 and 24). Therefore, we used the data of Satyro et al.[3] for the solubility of water in hexadecane (n=16) : $c_s = 8.6704\ 10^{-4}$ water mole fraction at 20°C or 0.0531kg.m^{-3}. And data of Su et al.[4] for the diffusion coefficient of water in hexadecane: $D_{wo} = 1.15\ 10^{-9}$ m^{2}s^{-1}.

In the experiments presented here, we do not know the water concentration in oil (c_∞). We thus need to estimate Δc for our experimental conditions, which is not obvious: here again there is no data in the literature relating water content in oil in contact with ambient air in function of relative humidity (%RH). Thus, dividing the experimental $D_{wo}\Delta c$ obtained from

figure 3 by the $\mathbf{D_{wo}}$ from Satyro et al. gives us an estimation of $\mathbf{\Delta c}$. We then found that $\mathbf{c_\infty}$=0.0414 kg.m^{-3} (41.4mgL^{-1}), corresponding to a relative undersaturation of 78%. Link with ambient air %RH still have to be made. However, this estimate of $\mathbf{\Delta c}$ is coherent with our experimental condition, in which oil is in contact with ambient air at HR~50% and provides confidence in our interpretation.

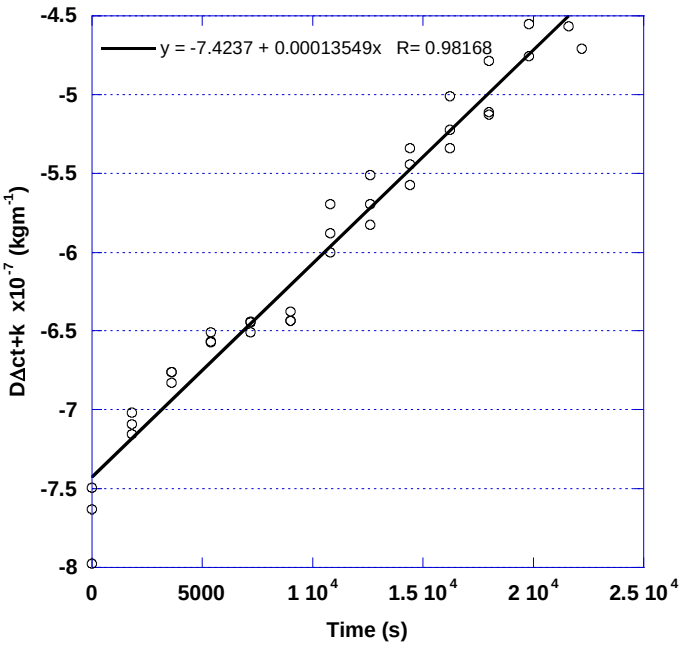

Figure S3: Test of Constant contact radius mode with diffusion-controlled evaporation (eq.20 reference [2])

COMPUTING CONTACT ANGLE OF THE MICRODROPLET WITH THE SUBSTRATE, MICRODROPLET HEIGHT, CONTACT DIAMETER AND MICRODROPLET VOLUMES : In this section we compute contact angle of the microdroplet with the substrate, microdroplet height, contact diameter and microdroplet volumes. First, droplets are considered symmetric around a central vertical axis: i.e. whatever direction the drop is viewed from.

Second, the contact area of the droplets with the substrate is considered as a circular surface. Despite this, there are small differences in shape because droplets are generated while the tip of the injector is moving (figure S4b). These fluctuations from a circular contact area are supposed to have a negligible effect on contact angle and droplet volume. Lastly, we assume there is no shape distortion due to gravity; thus microdroplet profiles can be fitted to a segment of a circle.

Contact angle (θ) and volume (**V**) of a droplet are estimated from the measurement of **H** (microdroplet height), **W** (microdroplet width), **D**(contact diameter), **R** (microdroplet radius) and **h** (defined in fig.Ac-d)

The volume of a sessile microdroplet having a contact angle θ with the surface is given by:

$$\mathbf{V} = \frac{\pi \times \mathbf{R}^3}{3} \times (2 + \cos\theta) \times (1 - \cos\theta)^2 \qquad \text{(S3)}$$

1. Under non-wetting condition, when θ >90° (fig.S4c), $\mathbf{R} = \frac{\mathbf{W}}{2}$, **H = R+h** and θ is the complementary angle of δ

($\theta + \delta = \pi$) thus $\cos\theta = \cos(\pi - \delta) = -\cos\delta$

with $\cos\delta = \frac{\mathbf{h}}{\mathbf{R}}$

Finally $\theta = \arccos(-\frac{\mathbf{h}}{\mathbf{R}})$ (S4)

when θ>90° the contact diameter is calculated from :

$$\mathbf{D} = 2 \times \sqrt{\mathbf{R}^2 - \mathbf{h}^2} \tag{S5}$$

2. Under wetting condition, when θ<90°, **D=W** and **h=H**(fig.S4d)

$$\mathbf{R} = \frac{\mathbf{a}^2 + \mathbf{h}^2}{2 \times \mathbf{h}} \tag{S6}$$

With $\mathbf{a} = \frac{\mathbf{W}}{2}$ and $\boldsymbol{\theta} = \mathbf{arcsin}(\frac{\mathbf{a}}{\mathbf{R}})$ (S7)

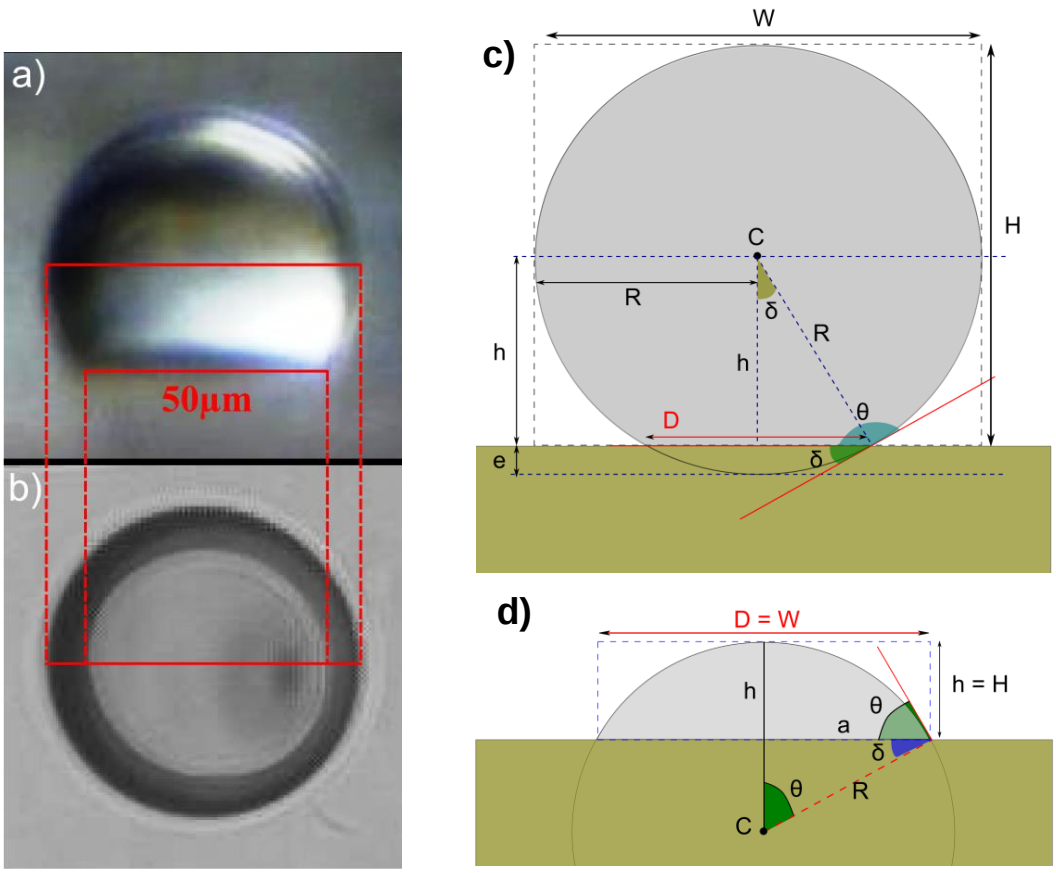

Figure S4: (a) Side view and (b) top view of 2.71M NaCl microdroplets (151pL) in oil, Schematic representation of a sessile droplet and its parameters for the model in two possible cases: (c) **H ≥ R, θ**>90° under non-wetting and (d) **R>H, θ**<90° under wetting conditions.

REFERENCES

(1) Picknett, R. G.; Bexon, R., The evaporation of sessile or pendant drops in still air. *Journal of Colloid and Interface Science* **1977,** 61, (2), 336-350.

(2) Mchale, G.; Aqil, S.; Shirtcliffe, N. J.; Newton, M. I.; Erbil, H. Y., Analysis of Droplet Evaporation on a Superhydrophobic Surface. *Langmuir* **2005,** 21, (24), 11053-11060.

(3) Satyro, M. A.; Shaw, J. M.; Yarranton, H. W., A practical method for the estimation of oil and water mutual solubilities. *Fluid Phase Equilibria* **2013,** 355, (0), 12-25.

(4) Su, J. T.; Duncan, P. B.; Momaya, A.; Jutila, A.; Needham, D., The effect of hydrogen bonding on the diffusion of water in n-alkanes and n-alcohols measured with a novel single microdroplet method. *The Journal of Chemical Physics* **2010,** 132, (4), 044506-8.

SYNOPSIS TOC